# Genome-wide DNA methylation changes in human spermatogenesis

Lara M. Siebert-Kuss,[1,7] Verena Dietrich,[2,7] Sara Di Persio,[1] Jahnavi Bhaskaran,[3,4,5] Martin Stehling,[5] Jann-Frederik Cremers,[6] Sarah Sandmann,[2] Julian Varghese,[2] Sabine Kliesch,[6] Stefan Schlatt,[1] Juan M. Vaquerizas,[3,4,5] Nina Neuhaus[1,8] and Sandra Laurentino[1,8*]

[1] Centre of Reproductive Medicine and Andrology, Institute of Reproductive and Regenerative Biology, University of Münster, Münster, Germany.

[2] Institute of Medical Informatics, University of Münster, Münster, Germany.

[3] MRC Laboratory of Medical Sciences, London, UK

[4] Institute of Clinical Sciences, Imperial College London, London, UK

[5] Max Planck Institute for Molecular Biomedicine, Münster, Germany

[6] Department of Clinical and Surgical Andrology, Centre of Reproductive Medicine and Andrology, University Hospital of Münster, Münster, Germany.

[7] These authors contributed equally

[8] Lead Contact

* Correspondence: Sandra.Laurentino@ukmuenster.de

**Running title:** DNA methylation during human spermatogenesis

## Summary

Sperm production and function require the correct establishment of DNA methylation patterns in the germline. Here, we examined the genome-wide DNA methylation changes during human spermatogenesis and its alterations in disturbed spermatogenesis. We found that spermatogenesis is associated with remodeling of the methylome, comprising a global-decline in DNA methylation in primary spermatocytes followed by selective remethylation, resulting in a spermatid-specific methylome. Hypomethylated regions in spermatids were enriched in specific transcription factor binding sites for DMRT and SOX family members and spermatid-specific genes. Intriguingly, while SINEs displayed differential methylation throughout spermatogenesis, LINEs appeared to be protected from changes in DNA methylation. In disturbed spermatogenesis, germ cells exhibited considerable DNA methylation changes, which were significantly enriched at transposable elements and genes involved in spermatogenesis. We detected hypomethylation in SVA and L1HS in disturbed spermatogenesis, suggesting an association between the abnormal programming of these regions and failure of germ cells progressing beyond meiosis.

## Keywords

DNA methylation, epigenetics, germline, human spermatogenesis, infertility, male germ cells, methylome, transposable elements

## Introduction

There is growing evidence that the establishment of the male germ cell methylome is not restricted to embryonic development, but continues in adulthood during spermatogenesis (Oakes *et al*, 2007; Langenstroth-Röwer *et al*, 2017; Di Persio *et al*, 2021a; El Omri-Charai *et al*, 2023; Huang *et al*, 2023). Especially in the early phases of meiosis, when replication and recombination occur, the genome is hypomethylated. This event is highly conserved between mouse and human and has been hypothesized to result from a delay in DNA methylation maintenance (Gaysinskaya *et al*, 2018; Huang *et al*, 2023). Still, there is limited information on DNA methylation during human spermatogenesis or whether disturbances in this process impact spermatogenesis and sperm function.

Epigenetic remodeling, which includes reprogramming of the methylome, is essential for cell-fate decisions in mammals (Klemm *et al*, 2019; Markenscoff-Papadimitriou *et al*, 2020; Izzo *et al*, 2020). Recently, it has been demonstrated that the impaired function of enzymes involved in the DNA methylation machinery results in a range of disturbances to spermatogenesis, including complete sterility (Bourc'his *et al*, 2001; Zamudio *et al*, 2015; Barau *et al*, 2016; Karahan *et al*, 2021; Dura *et al*, 2022). In most cases of severe male infertility, sperm output is drastically reduced and the etiology is unknown (Tüttelmann *et al*, 2018). In particular, cryptozoospermia is characterized by a drastic decline in germ cells going through meiosis and an accumulation of the most undifferentiated spermatogonia (Di Persio *et al*, 2021b). Previously, we reported aberrant DNA methylation in bulk germ cells of men displaying cryptozoospermia (Di Persio *et al*, 2021a), which led us to hypothesize that aberrant DNA methylation could be the underlying cause. However, the extent to which the different germ cell types carry altered DNA methylation, the genomic regions affected, and their involvement in post-meiotic germ cell decline, remain to be assessed.

Especially during meiosis, the genome heavily depends on the suppression of transposable elements (TEs). This is usually achieved by epigenetic mechanisms such as gene-silencing histone modifications, piRNA machinery, and DNA methylation (Zamudio & Bourc'his, 2010,

Zamudio et al 2015). Thus, the suppression of TEs, such as long and short-interspersed nuclear elements (LINE/SINE), is crucial to maintain genome integrity in the germline (Schaefer *et al*, 2007; Vaissiere *et al*, 2008; Zamudio & Bourc'his, 2010; Dong *et al*, 2019), which, when lost, leads to sterility in mice (Barau *et al*, 2016; Vasiliauskaitė *et al*, 2018). Differential methylation at TEs or dysfunctional TE silencing pathways have been linked to male infertility (Bourc'his & Bestor, 2004; Carmell *et al*, 2007; Aravin *et al*, 2007; Heyn *et al*, 2012; Urdinguio *et al*, 2015). Importantly, different TEs have different modes of DNA methylation acquisition (Fukuda et al 2022), and evolutionary younger (SINE-VNTR-Alus (SVAs)) TEs are protected from genome-wide methylome erasure during development (Seisenberger *et al*, 2012; Kobayashi *et al*, 2012; Gkountela *et al*, 2015; Guo *et al*, 2015), indicating that these elements are especially hazardous to the genome and must be protected via DNA methylation. The protective role of DNA methylation at different TEs in germ cells during spermatogenesis and its association with male infertility, in particular during the hypomethylated phase of meiosis, remains to be elucidated.

By performing whole methylome analysis on pure human male germ cell fractions, we uncovered that human spermatogenesis is associated with epigenetic remodeling of the methylome. We found that the global decline in DNA methylation in primary spermatocytes is followed by selective remethylation in specific regions in spermatids, suggesting that the hypomethylated primary spermatocyte genome is not exclusive a transient side effect of DNA replication but is required for the establishment of a spermatid-specific methylome. We found significant differences in DNA methylation in germ cells of infertile men, particularly occurring in intergenic regions and TEs, and demonstrate that different TEs are differentially reprogrammed during spermatogenesis. Our study increases current evidence on the role of DNA methylation changes during human spermatogenesis, and points to an association between altered DNA methylation and spermatogenic failure.

# Results

## Primary spermatocytes exhibit genome-wide reduced DNA methylation levels

To investigate genome-wide DNA methylation changes during human spermatogenesis, we performed whole-genome enzymatic methyl-sequencing (EM-seq) on isolated human male germ cells. We obtained undifferentiated spermatogonia (2C/MAGEA4$^{+}$/UTF1$^{+}$/DMRT1$^{-}$; Undiff), differentiating spermatogonia (2C/MAGEA4$^{+}$/UTF1$^{-}$/DMRT1$^{+}$; Diff), primary spermatocytes (double-diploid cells; 4C), and spermatids (haploid cells; 1C) from men with normal spermatogenesis (controls, CTR) (Fig. 1A, Supplementary Fig. S1A). We captured an average of 28,049,115 CpG sites per sample, including 26,861,322 CpGs with a minimum coverage of 5 reads, which were the ones considered for further analyses.

To guarantee that all germ cell fractions were free of somatic DNA, we compared the methylation of published sperm-soma differentially methylated regions (DMRs) (Leitão *et al*, 2020) in our germ cell fractions with those published for sperm and blood samples (Laurentino *et al*, 2020). We confirmed male germ cell-specific methylation in the isolated cell fractions (Supplementary Fig. S1B). Interestingly, the methylation patterns of 50 known maternally and paternally methylated imprinted control regions (ICRs) (Monk *et al*, 2018) were also similar to those found in sperm and had the same methylation pattern in all germ cell types (Fig. 1B, Supplementary Table S1). Analysis of global DNA methylation levels across spermatogenesis revealed comparably high average levels (>74%) of DNA methylation in undifferentiated spermatogonia, differentiating spermatogonia, and spermatids (Fig. 1C), which is consistent with the characteristically high DNA methylation levels in male germ cells (Greenberg & Bourc'his, 2019). Intriguingly, the global DNA methylation levels in primary spermatocytes were significantly lower, with a mean of 66% (Fig. 1C), compared to all other germ cell types. To elucidate whether the DNA hypomethylation in primary spermatocytes occurs randomly in the genome or is specific to particular genomic features, we analyzed the DNA methylation in gene bodies and 5000 bp up- and downstream of the transcriptional start (TSS) and end sites (TES). Our data showed that the decreased DNA

methylation in primary spermatocytes, which was evident at TSS and TE, and was particularly prominent in gene bodies (Fig. 1D). Deeper analysis of the different genomic compartments revealed a decline in DNA methylation in primary spermatocytes that occurred across untranslated regions (UTRs), transcripts, and RNA repeats. DNA methylation also declined at long terminal repeats (LTRs), including the TEs LINEs and SINEs, indicating a genome-wide demethylation in primary spermatocytes (Fig. 1E). In contrast, there was no change in DNA methylation at centromeric and satellite regions, which overall display low DNA methylation levels in all germ cell types evaluated.

**Differentially methylated regions during spermatogenesis are enriched at SINE repeats**

In order to identify regions that change their DNA methylation during spermatogenesis, we compared the methylomes of the different germ cell-types (coverage ≥ 5, p-value ≤ 0.05 (metilene), difference ≥ 20 %) using metilene and camel (Wöste *et al*, 2020). Applying stringent filtering, we identified a total of 16,000 DMRs throughout the different germ cell types (Fig. 2A, Supplementary Table S2). We found the fewest DMRs between undifferentiated and differentiating spermatogonia (64 DMRs, mean Δ methylation =24%), indicating a high level of similarity between the methylomes of the two spermatogonial subpopulations. The most DMRs were detected between spermatogonia (undifferentiated and differentiating) and primary spermatocytes (5212 and 5487 DMRs, mean Δ methylation = 22% and 23%). When we compared the cell types corresponding to the least and most differentiated cell types, namely undifferentiated/differentiating spermatogonia and spermatids, we found the most extreme changes in DNA methylation (1516 and 1001 DMRs, mean Δ methylation = 41% and 36%). Analyses on the intersection of DMRs with genes or promoters revealed that 53 - 70% are associated with genes and 3 - 9% with a promoter (Fig. 2B). To investigate the features of the DMRs we analyzed their CpG enrichment and length. In comparison to other cell type comparisons that had an average of 8 CpGs and a length of 340 bp, we found that DMRs obtained from the comparisons that included primary spermatocytes were the longest (average 975 bp) and the most enriched in CpGs (average

14 CpGs) (Fig. 2C+D). We asked whether certain chromosomes showed an enrichment in DMRs. To this end, we normalized the number of DMRs per chromosome size (bp) (Piovesan *et al*, 2019) and scaled for the number of DMRs per group comparison. We found that DMRs were similarly distributed across the different chromosomes in all comparisons, except for the 64 undifferentiated vs differentiating spermatogonia DMRs, which showed a peak on the X chromosome (Fig. 2E). Moreover, we sought to elucidate whether the DMRs are significantly enriched for certain genomic features. Intriguingly, enrichment analysis showed that particularly DMRs of the undifferentiated spermatogonia vs spermatids comparison, were significantly enriched (corrected p-value ≤ 0.00019, z-score >0) at CpG shelves, 3'UTRs, and exons, indicating changes in DNA methylation in these regions might be characteristic of the process of spermatogenesis (Fig. 2F). We found reduced global DNA methylation levels of LINEs and SINEs exclusively in primary spermatocytes (Fig. 1E). For all DMRs between the different germ cell types, we found a significant enrichment only at SINEs (Fig. 2F), suggesting a role for DNA methylation changes in SINEs during spermatogenesis. In contrast, we found an underrepresentation compared to what would be expected by chance (z-score < 0) of promoters, CpG shores and islands in DMRs of the differentiating vs primary spermatocyte comparison, putatively indicating the methylation levels of these regions are maintained during the entry into meiosis. Interestingly, LINE elements were underrepresented in the linear DMR comparisons (i.e. Undiff vs Diff, Diff vs 4C, 4C vs 1C) as well as between the undifferentiated spermatogonia vs primary spermatocyte comparison, indicating a preferential DNA methylation retention at LINE repeat regions during spermatogenesis.

To unravel the putative regulatory role of DNA methylation changes in biological processes in the respective germ cell types, we investigated the nearby genes with a regulatory region within the identified DMRs. We found that the DMRs of all comparisons overlapped a putative regulatory region of 29 to 1685 genes (Supplementary Table S3). Within these genes, gene ontology (GO) analysis revealed an enrichment of distinct GO terms in biological processes (BP) and molecular functions (MF), such as regulation of cation channel

activity (Undiff vs Diff), and GTPase regulatory activity (Undiff vs 1C) (Supplementary Fig. S2) indicating changes in DNA methylation during spermatogenesis associates with specific cellular functions.

**Hypomethylated regions in spermatids are enriched for TF binding sites**

Local methylation changes can identify potential regulatory regions in developing germ cells (Kubo *et al*, 2015). To address whether regulatory transcription factor (TF) binding sites are subject of changes in DNA methylation during spermatogenesis, we analyzed the DMRs for their enrichment in TF binding motifs by applying the Hypergeometric Optimization of Motif Enrichment (HOMER) analysis. This analysis revealed that particularly the DMRs of the spermatogonia (undifferentiated and differentiating) vs spermatids comparisons were enriched for motifs recognized by TFs such as *DMRT1*, *DMRT6/ DMRTB1,* and *SOX6* (Fig. 3A). To assess whether these TFs are expressed in the respective germ cell types, in which we found differential methylation of their motifs, we analyzed their expression during spermatogenesis in our published scRNA-seq dataset (Di Persio *et al*, 2021b). We found germ cell type-specific expression of *DMRT1*, *DMRTB1,* and *SOX6* in differentiating spermatogonia, spermatocytes, and spermatids, respectively (Fig. 3B), suggesting the change in DNA methylation of the identified motifs is a feature of spermatogenesis.

**Germ cell type-specific expression of the DMR associated genes**

Low or unmethylated regions frequently mark accessible chromatin regions (Stadler *et al*, 2011). As we found that the methylomes of spermatids, when compared to undifferentiated spermatogonia, have the highest number of hypomethylated DMRs and are enriched for TF binding sites, we hypothesized that the hypomethylated DMRs mark functionally important regions for spermatids. To this end we evaluated whether the DMR associated genes (overlapping a gene body) of the undifferentiated spermatogonia vs spermatids comparison have specific expression in spermatids. Indeed, we identified 24 highly spermatid-specific genes (e.g. *RAD21L1, KLK11, FEM1B, CLPB, NRDC*) among the hypomethylated DMRs

(Fig. 4A). Intriguingly, and in line with the association of gene expression and gene body methylation (Ball *et al*, 2009), we found 41 spermatogonial-specific genes (e.g. *SERPINE2, BLVRA, TJP1, YPEL2, TCF3*) that have a hypermethylated DMR in their gene bodies in undifferentiated spermatogonia (Fig. 4A). When we analyzed the DMR associated genes of other group comparisons, we observed that the majority of germ cell type-specific genes are hypermethylated (Supplementary Fig. S3A) and only a minority of them are hypomethylated in the respective germ cell types (Supplementary Fig. S3B).

Retained nucleosomes in human sperm were shown to be enriched at gene regulatory regions (Hammoud *et al*, 2009; Brykczynska *et al*, 2010). To examine whether the hypomethylated DMRs of the undifferentiated spermatogonia vs spermatids comparison mark regulatory active regions in sperm, we analyzed the overlap of the hypomethylated DMRs with retained histone marks in sperm. Indeed, overlap analysis with publicly available datasets on human sperm histones (GSE40195) revealed that ~17% of DMRs overlapped with a retained histone mark in sperm (Supplementary Table S4). The active histone mark H3K36me3 overlaid 10% of the hypomethylated DMRs in spermatids. Although H3K36me3 is associated with gene body methylation to maintain gene expression stability (Sharda & Humphrey, 2022), we found H3K36me3 marked a hypomethylated region in *AGPAT3*, which is specifically expressed in spermatids (Fig. 4B).

**Disturbed spermatogenesis displays methylome changes at TEs and spermatogenesis genes**

Aberrant DNA methylation was found in sperm of infertile men, particularly in imprinted genes (Marques *et al*, 2004; Poplinski *et al*, 2010; Kläver *et al*, 2013; Kuhtz *et al*, 2014; Laurentino *et al*, 2015; Urdinguio *et al*, 2015). To confidently associate changes in DNA methylation with male infertility, it is important to exclude effects of differential methylation, especially in imprinted genes, due to potential contamination with somatic DNA. Accordingly, it remains to be elucidated whether genome-wide changes in germ cells of infertile patients occur. To this end, we analyzed methylomes of germ cells isolated from testicular tissues of

men diagnosed with cryptozoospermia (CZ) (Fig. 5A). Ploidy analysis confirmed the characteristic cryptozoospermic-phenotype (Di Persio *et al*, 2021b), consisting of a decreased proportion of spermatids in comparison to the CTR samples (Fig. 5B). Based on cell numbers (Supplementary Table S5), we were able to generate methylomes of undifferentiated spermatogonia, differentiating spermatogonia, and primary spermatocytes from these samples. Quality control (Leitão *et al*, 2020; Di Persio *et al*, 2021a) indicated the presence of somatic DNA in CZ-1 (Supplementary Fig. 4A+B), therefore we exclude all fractions from this patient from further analyses. The other two samples were free of somatic DNA and, except for one secondary ICR (MKRN3:TSS-DMR) that showed an isolated increase in DNA methylation (average of 35%), showed no overall imprinting errors (Supplementary Fig. S4C, Supplementary Table S6).

To examine whether regions exhibit differential methylation in cryptozoospermic patients (n=2) compared to control patients (n=3), we analyzed potential DMRs between undifferentiated spermatogonia, differentiating spermatogonia, and primary spermatocytes. We applied the same DMR filtering as for the control germ cell DMRs (coverage ≥ 5, p-value ≤ 0.05 (metilene), difference ≥ 20 %) but, due to the smaller sample size, we used stricter filtering parameters for the methylation range within the cryptozoospermic group (range ≤ 15%) to filter out DMRs potentially influenced by the genetic background. We found 107, 144, and 152 DMRs (mean $\Delta$ methylation = 31-37%) in undifferentiated spermatogonia, differentiating spermatogonia, and primary spermatocytes between CTR and CZ samples (Fig. 5C). We found few overlapping DMRs between all comparisons (Supplementary Table S7). The DMRs were overall enriched in chromosomes 21 and X (Fig. 5D) and significantly enriched in intergenic regions and at retroposons (Fig. 5E), indicating that altered DNA methylation patterns in cryptozoospermic germ cells are predominantly affecting these regions. Particularly hypomethylation of evolutionary young TEs have been associated with decreased fertility in mice (Karahan *et al*, 2021). Therefore, we examined whether we find changes in DNA methylation in evolutionary younger (SVA D/F, L1Hs, and L1PA2-5) and older TEs (HERVH-int and L1M7) between control and cryptozoospermic patients. We found

that spermatogonia (undifferentiated and differentiating) and primary spermatocytes of cryptozoospermic men had a decrease in methylation in SVA D/F TEs (Fig. 5F). When we analyzed the methylation levels of different TEs in each control and cryptozoospermic sample, we found that the hypomethylation in TEs of the cryptozoospermic group is driven by sample CZ-2, which showed hypomethylation not only in SVA D/F, but also in SVA B/C as well as L1HS, L1PA2, HERVH-int (Supplementary Fig. S5). Interestingly, SVA A TEs were hypermethylated in both cryptozoospermic samples and in all control samples.

In bulk germ cells of cryptozoospermic samples, changes in DNA methylation were associated with functionally relevant genomic regions (Di Persio *et al*, 2021a). Our analysis revealed that CTR/CZ DMRs are associated with putative regulatory regions of 29, 39, and 38 genes in undifferentiated spermatogonia, differentiating spermatogonia, and primary spermatocytes, respectively (Supplementary Table S8), which were significantly enriched for genes involved in differentiation processes (e.g. cell morphogenesis involved in differentiation) (Supplementary Fig. S4D). As we found 29 - 40 % of DMRs overlap a gene body (Supplementary Fig. S4E), we asked whether they associate with germ cell type-specific gene expression, potentially pointing to a relevant function for spermatogenesis. Gene expression analysis showed that 25 - 33% DMR associated genes overlap with genes specifically expressed by spermatogonia (*AL157778.1, PCDH11X, EDA, ANKRD33B, AC087354.1, DACH2, VPS37D*), spermatocytes (*HSPBAP1, FOXK1, ARHGAP33, NBPF1, SLCO3A1*), or spermatids (*CCDC200, AL589935.1, ADARB2, SNHG27*) (Supplementary Fig. S4F). In summary, although we could not detect overall changes at ICRs, we found that cryptozoospermic germ cells exhibit changes in DNA methylation particularly occurring at evolutionarily younger TEs of the SAV familiy and at spermatogenic genes.

## Discussion

The establishment of the germ cell methylome extends beyond prenatal development (Oakes *et al*, 2007; Langenstroth-Röwer *et al*, 2017; Di Persio *et al*, 2021a; El Omri-Charai *et al*, 2023; Huang *et al*, 2023). In this study, we used whole methylome sequencing of germ cells to identify changes in DNA methylation occurring during human spermatogenesis. This included demethylation in primary spermatocytes followed by remethylation of specific regions, resulting in a unique spermatid-specific DNA methylation pattern. Furthermore, we identified changes in the DNA methylation of germ cells from infertile men particularly affecting intergenic regions and TEs.

Previous studies have reported that the male germline genome becomes hypomethylated during meiosis. They hypothesized that this decline in methylation is due to a delay in DNA methylation maintenance (Gaysinskaya *et al*, 2018) and is associated with meiotic recombination (Huang *et al*, 2023). Here, we show that the demethylation occurring in human male meiosis affects gene bodies and genomic repeats similarly, but not centromeres and satellite regions. Our data supports the hypothesis of a replication-dependent passive DNA demethylation in early meiosis resulting in a hypomethylated genome in spermatocytes (Gaysinskaya *et al*, 2018; Huang *et al*, 2023). This phase is followed by an increase in average DNA methylation to levels similar to those prior to meiosis. However, careful examination of regions showing differential methylation demonstrates that discrete regions remain protected from re-methylation in spermatids. This indicates that genome-wide re-methylation in spermatids is not an outcome of DNA maintenance machinery restoring CpG methylation after meiosis, but instead evidences the establishment of a highly specific DNA methylation pattern in spermatids.

Our findings lead us to hypothesize that a functional relationship exists between the establishment of a spermatid-specific methylome and gene expression during spermatogenesis. This notion was reinforced by our finding that hypomethylated regions in spermatids retain active histones in sperm. These regions correspond to genes specifically

expressed by spermatids. Our hypothesis is further corroborated by analogous results in rodents, which demonstrate that the spermatid methylome undergoes differential methylation during spermiogenesis and is enriched for regulatory binding sites when compared to spermatogonial stem cells (Kubo *et al*, 2015; El Omri-Charai *et al*, 2023).

During normal human spermatogenesis, we showed that primary spermatocytes were the only germ cell type displaying a global decrease in DNA methylation at LTRs, LINEs, and SINEs. The silencing of TEs is crucial for maintaining genome integrity and usually achieved by epigenetic modifications, including repressive histone modifications and DNA methylation (Zamudio & Bourc'his, 2010). In line with this, our data showed that LINEs are significantly underrepresented among the regions with differential methylation, indicating that the methylation status of LINEs is protected in adult male germ cells. In contrast, we found that DNA methylation at SINEs significantly changes in all germ cell types during spermatogenesis, indicating that these regions are not under the same tight regulation as LINEs. Consistent with our data on genome-wide DNA methylation changes at SINE elements, a recent study found varying levels of SINE methylation in sperm, specifically at promoters of spermatogenic genes (Lambrot *et al*, 2021). Considering our data and the role of TEs in the regulation of genes (Zamudio & Bourc'his, 2010; Sasaki *et al*, 2008), we hypothesize that SINE methylation might play a regulatory role in human spermatogenesis.

Mice deficient for genes belonging to the DNA methylation machinery display male infertility or sterility (Bourc'his *et al*, 2001; Zamudio *et al*, 2015; Barau *et al*, 2016; Karahan *et al*, 2021; Dura *et al*, 2022). In humans, the hypothesis that male infertility is associated with aberrations in DNA methylation was first explored by numerous studies reporting epimutations in the sperm of infertile men (Åsenius *et al*, 2020), a notion that was somewhat challenged by our findings that somatic DNA artifacts and gene variants may have confounded previous studies (Leitão *et al*, 2020). However, more recently we identified consistent DNA methylation changes in testicular germ cells, but not in sperm, of infertile men, indicating that DNA methylation abnormalities during spermatogenesis might in fact be associated with disturbed spermatogenesis (Di Persio *et al*, 2021a). Here, we have

expanded on this by identifying clear changes in DNA methylation at specific steps of spermatogenesis in germ cells of infertile men. Intriguingly, although these changes were germ cell type-specific, the affected regions were consistently enriched in TEs and predominantly localized on chromosomes 21 and X, chromosomes associated with monogenic disorders and male germ cell differentiation (Soumillon *et al*, 2013; Sangrithi *et al*, 2017; Ernst *et al*, 2019). In one of the cryptozoospermic samples, we specifically found hypomethylated SVA elements, together with hypomethylated L1HS, which is required to express SVA elements (Raiz *et al*, 2012). This finding shows similarities with a study demonstrating an association between hypomethylated young TEs and male infertility in mice (Karahan *et al*, 2021). DNA methylation is one of the main repressors of TE expression (Schaefer *et al*, 2007; Vaissiere *et al*, 2008; Zamudio & Bourc'his, 2010; Dong *et al*, 2019). Therefore, we hypothesize that the protection of evolutionary young TEs of the SVA family is disrupted in this patient's germline leading to genomic instability due to the expression of SVAs and a phenotype of disturbed spermatogenesis. However, limited material prevents us from substantiating this at transcriptional level. Our findings on aberrant TE methylation in germ cells of men with cryptozoospermia are, nevertheless, supported by studies showing that loss of DNA methylation at TEs results in sterility in mice (Barau *et al*, 2016; Vasiliauskaitė *et al*, 2018). Failure in TE silencing affects germline gene expression in mice (Vasiliauskaitė *et al*, 2018) and, especially during meiosis, can lead to meiotic arrest (Bourc'his & Bestor, 2004; Carmell *et al*, 2007; De Fazio *et al*, 2011). In cryptozoospermic patients, some seminiferous tubules show complete spermatogenesis while others display spermatogenic arrest (Di Persio *et al*, 2021b). This heterogeneous phenotype could be caused by epimutations in the germline, in contrast to genetic variations that usually lead to complete phenotype penetrance. In line with this, we found that numerous infertility-related DMR associated genes are expressed during spermatogenesis (e.g. *VPS37D, FAM9B, SLCO3A1, CCDC200*).

In conclusion, our findings provide an unprecedented view of genome-wide DNA methylation changes during human spermatogenesis, highlighting the role of DNA methylation,

358 particularly at TEs, during this process, and indicating a potential role for altered TE
359 methylation in the etiology of human male infertility.

## 360 Acknowledgments

361 We thank the Cologne Center for preparing the sequencing libraries and performing the
362 sequencing. We appreciate the excellent technical support in patient material collection,
363 histological evaluation of the testicular tissues and hormone measurement by Nicole Terwort,
364 Sabine Forsthoff, Heidi Kersebom, Elke Kößer and Elisabeth Lahrmann as well as help from
365 the andrology lab (CeRA). Panels Fig. 1A and Fig. 5A were created with BioRender.com.

366 This study was carried out within the frame of the Deutsche Forschungsgemeinschaft (DFG,
367 German Research Foundation) sponsored Clinical Research Unit 'Male Germ Cells'
368 (CRU326, project number LA 4065/3-2 & NE 2190/3-2 to NN & SL) & Innovative Medical
369 Research (IMF) of the Medical Faculty of the University of Münster (to SDP).

## 370 Author contributions

371 Study design: NN, SL; Conceptualization: LS, VD, NN, SL; Patient counseling: JC, SK; Data
372 curation: LS, JB, MS, JC, SK; Formal analysis: LS, VD, SDP, MS; Investigation: LS, VD,
373 SDP, JMV, NN, SL; Supervision: StS, SaS, JV, SK, JMV, NN, SL; Funding acquisition: SDP,
374 JMV, NN, SL; Writing original draft: LS, VD, NN, SL; Writing review & editing: all authors.

375 All authors approved the final version of the manuscript.

## 376 Declaration of interests

377 The authors declare no competing interests.

378

# Figure titles/ legends

**Fig. 1: Primary spermatocytes exhibit genome-wide reduced DNA methylation levels.** **A** Schematic illustration on the retrieval of whole genome methylome data from germ cells of samples with normal spermatogenesis (control, CTR). CpGs refer to the mean CpG number captured by enzymatic methyl-sequencing in all germ cell fractions (n=12). **B** Lineplot depicts the methylation in 50 imprinted control regions (ICRs) for each CTR sample and germ cell type compared to published blood and sperm samples (Laurentino *et al*, 2020). **C** Box plots display the mean global DNA methylation levels. Statistical tests: ANOVA test followed by Tukey-HSD-test: *** < 0.001 of 4C compared to all other germ cells. Data are represented as median (center line), upper/ lower quartiles (box limits), 1.5 x interquartile range (whiskers). **D** Lineplot shows mean methylation levels per group across gene bodies divided into 50 intervals (bins) and 5 kb upstream and downstream of the transcriptional start sites (TSSs) and transcriptional end sites (TESs). **E** Violin plots represent methylated CpGs across different genomic compartments. Panel A was created with BioRender.com. See also Supplementary Fig. S1.

**Fig. 2: Differentially methylated regions during spermatogenesis are enriched at SINE repeats**. **A** Heatmaps display methylation values and CpG numbers of the differentially methylated regions (DMRs) of all germ cell type comparisons. **B** DMRs are associated with genes and promoters. **C** Frequency of CpG number per DMR within the different group comparisons. **D** Violin plot depicts distribution of the DMR width in each group comparison. **E** Distribution of DMRs per chromosome scaled for chromosomal size (basepairs) and normalized by their total count within one group. **F** Enrichment of DMRs for general genomic features and genomic repeats. Positive and negative enrichments are indicated by z-score. Displayed annotations, p < 0.00019 by permutation tests. Color coding of the group comparisons are depicted in panel A.

**Fig. 3: Hypomethylated regions in spermatids are enriched for specific TF binding sites**. **A** Depicted are the enriched sequences of known motifs identified by HOMER. HOMER analysis was run for all DMR comparisons and significant results are displayed (p-value < 0.01, FDR <0.05). **B** Dot plots show the average single cell expression (Di Persio *et al*, 2021b) of the top 3 transcription factors (TF) with enriched motifs among the DMRs identified with HOMER. SPC = spermatocytes, SPD = spermatids.

**Fig. 4: Hypomethylated regions in the spermatid methylome mark spermatid-specific genes. A** Single cell expression (Di Persio *et al*, 2021b) of hypomethylated DMR associated genes with specific expression in spermatids and hypermethylated DMR associated genes with specific expression in undifferentiated spermatogonia of the undifferentiated spermatogonia vs 1C DMRs. **B** Example of the DMR methylation within the *AGPAT3* locus that is hypermethylated in Undiff and Diff and hypomethylated in 4C and 1C and specifically expressed in SPD. H3K36me3 histone modification data (GSE40195) in human sperm is also shown. SPC = spermatocytes, SPD = spermatids. See also Supplementary Fig. S3.

**Fig. 5: Disturbed spermatogenesis displays methylome changes at TEs and spermatogenesis genes**. **A** Schematic illustration on the retrieval of whole genome methylome data of germ cells from samples with disturbed spermatogenesis (cryptozoospermia, CZ). **B** Box plots show the proportion of cell types among the sorted cells in the CTR and CZ patients. Data are represented as median (center line), upper/ lower quartiles (box limits), 1.5 x interquartile range (whiskers). **C** Heatmaps display methylation values of the differentially methylated regions (DMRs) between CTR and CZ of the same cell type (Undiff vs Undiff, Diff vs Diff, 4C vs 4C). **D** Distribution of the CTR/CZ DMRs per chromosome scaled for chromosomal size (basepairs) and normalized by their total count within one group. **E** Enrichment of CTR/CZ DMRs for functional general genomic regions and genomic repeats. Positive and negative enrichments are indicated by z-score. Displayed annotations, p < 0.00019 by permutation tests. **F** Violin plots showing the CpG methylation of evolutionary younger (white boxes: L1Hs, L1PA2-5, and SVA_D/F) and older (grey boxes:

HERVH-int and L1M7) TEs in CTR and CZ germ cells. Color coding of the group comparisons are depicted in panel B. Panel A created with BioRender.com. See also Supplementary Fig. S4 and S5.

## Tables with titles and legends

N/A

## Materials & Methods

### Ethical approval

Patients included in this study underwent surgery for (microdissection) testicular sperm extraction (mTESE; n=6) at the Department of Clinical and Surgical Andrology of the Centre of Reproductive Medicine and Andrology, University Hospital of Münster, Germany. Each patient gave written informed consent (ethical approval was obtained from the Ethics Committee of the Medical Faculty of Münster and the State Medical Board no. 2008-090-f-S) and one additional testicular sample for the purpose of this study was obtained. Tissue proportions were snap-frozen or fixed in Bouin's solution.

### Selection and clinical evaluation of the patient cohort

All patients included in this study underwent full physical examination, hormonal analysis of luteinizing hormone (LH), follicle stimulating hormone (FSH), and testosterone (T), semen analysis (World Health Organization, 2010) and genetic analyses of the karyotype and screening for azoospermia factor (AZF) deletions. All patients had normal karyotypes (46,XY) and no AZF deletions. Exclusion criteria were biopsies of testis with germ cell neoplasia, a history of cryptorchidism of the biopsied testis, and acute infections. To study qualitatively and quantitatively normal spermatogenesis, we collected biopsies from control patients (CTR) that were diagnosed with obstructive azoospermia due to anejaculation (CTR-1) or a congenital bilateral absence of the *vas deferens* due to *CFTR* gene mutations (CTR-2, CTR-

3). No sperm was found in the ejaculate but after mechanical dissection of the testicular tissues. To study severely disturbed spermatogenesis, we collected biopsies from cryptozoospermic patients (CZ-1, CZ-2, CZ-3) that were diagnosed with hypergonadotropic oligoasthenoteratozoospermia and presented <0.1 Million sperm in the ejaculate after centrifugation. All CZ patients had elevated FSH levels (Supplementary Table S9).

**Histological analysis of the human testicular biopsies**

As a routine diagnostic procedure in our clinic, two testicular biopsies per testis were fixed in Bouin`s solution, the tissues were washed in 70% ethanol, embedded in paraffin, and sectioned at 5 µm. For histological evaluation, two independent testicular sections from each testis were stained with periodic acid-Schiff (PAS)/ hematoxylin and were evaluated based on the Bergmann and Kliesch scoring method (Bergmann & Kliesch, 2010) as previously described (Siebert-Kuss *et al*, 2023).

**Preparation of single-cell suspensions from testicular biopsies**

For the extraction of pure germ cell subtypes, testicular biopsies were digested into a single-cell suspension as previously published (Di Persio et al, 2021). The digestion was based on mechanically chopping up the testicular tissue with a sterile blade into ~ 1 $mm^3$ pieces and a two-step enzymatic incubation, first, with MEMα (ThermoFisher scientific, Gibco, Cat# 22561021) with 1 mg/ml collagenase IA (Merck/Sigma Aldrich, Cat# C9891) at 37 °C for 10 min and, second, with Hank's balanced salt solution (HBSS) containing 4 mg/ml trypsin (ThermoFisher scientific, Gibco, Cat# 27250018) and 2.2 mg/ml of DNase I (Merck/Sigma Aldrich, Cat# DN25) at 37 °C for 8 – 10 min and strong pipetting in between. Each enzymatic reaction was stopped by adding MEMα supplemented with 10% fetal bovine serum (FBS) (Merck, Cat# S0615) and 1% Penicillin/Streptomycin (ThermoFisher scientific, Gibco, Cat# 15140-148) and the supernatant discarded after centrifugation. Finally, cells were washed three times and the cell suspension then eliminated from erythrocytes by incubation in haemolysis buffer (0.83% NH4Cl solution) for three minutes. The reaction was stopped as

described above. Cell debris was removed by filtering the cell suspension through a 70 µm sterile CellTrics® filter (Sysmex). We used the trypan blue exclusion method for quantification of the obtained cell numbers. We incubated the cells (1 million cells / 1 ml HBSS) obtained after digestions with 1 µl Near-IR fluorescent reactive dyeLIVE/DEAD Fixable Dead Cell Stain Kit (Invitrogen; Cat: L34961; Ex: 633/635nm; Em: 775nm) for 30 min on ice and stopped the reaction by addition of 1 ml HBSS supplemented with 5% FBS. After centrifugation, unspecific antibody binding sites were blocked by incubation of the cells with HBSS containing 5% FBS for 45 min on ice. Following centrifugation, cells were fixed in Fix and Perm solution A for 30 min at room temperature and the reaction stopped as outlined above. After centrifugation, cell membranes were permeabilized by incubation with Fix and Perm solution B for 30 min at room temperature. After centrifugation 20% of cells were incubated with fluorophores-conjugated, unspecific immunoglobulin G (IgG) as negative controls, namely mIgG-AI647 (1:200, BioLegend, Cat# 400130), mIgG-Dy550 (1:20, Biolegend Cat#400166) and mIgG-Dy488 (1:20, BioLegend Cat#400166). The remaining cells were incubated with fluorophores-conjugated primary antibodies at room temperature for 1 h against DMRT1-AI647 (1:200, Santa Cruz, Cat# sc-377167 AF647), MAGEA4-Dy550 (1:20, Prof. G. C. Spagnoli, University Hospital of Basel, CH, conjugated) and UTF1-Dy488 (1:20, Merck/Millipore, Cat# MAB4337, conjugated). We used the Dylight™ 488 and 550 labeling kits (ThermoFisher, Cat# 53025 and CAT#84531) for conjugation of the IgGs, MAGEA4 and UTF1 antibodies, respectively. The antibody binding reaction was stopped by adding HBSS supplemented with 5% FBS. After centrifugation, cells were resuspended in HBSS containing 5% FBS and Hoechst (NucBlue® Live ReadyProbes® Reagent Protocol, R37605, Thermo Fisher) was added to distinguish the DNA contents of the cells.

**Fluorescence activated cell sorting analyses for isolation of human male germ cells**

For extraction of the different germ cell fractions, we applied a multi-parameter fluorescence activated cell sorting (FACS) strategy on the BD FACS Aria Fusion with FACSDiva software (v 8.02). We gated for cells and live cells based on the Near-IR fluorescent reactive dye

LIVE/DEAD™ (LIVE/DEAD™ Fixable Near-IR Dead Cell Stain Kit, Invitrogen, L10119). Spermatogonia were identified and gated within the diploid (2C) cells positive for the pan-spermatogonial marker MAGEA4. The 2C/ MAGEA4+ cells were further divided into undifferentiated spermatogonia (Undiff) and differentiating spermatogonia (Diff) by gating for $UTF1^{+}$/ $DMRT1^{-}$ and $UTF1^{-}$/ $DMRT1^{+}$ cells, respectively. Primary spermatocytes and spermatids were isolated and gated based on their DNA content for 4C and 1C cells, respectively. Cells were sorted with a 85 µm nozzle and collected in 200 µl HBSS containing 5% FBS. FACS data were analyzed using the FlowJo software (v 10.8.1).

**DNA isolation and enzymatic conversion of sorted testicular germ cells**

DNA was isolated from fixed and sorted cells using the MasterPure DNA purification kit (MC85200, Lucigen, LGC Ltd, Teddington, UK) following the manufacturer's protocol. We incubated the cells for 20 min at 90 °C prior to incubation with proteinase K at 65 °C for 1 h. DNA concentration was measured using Qubit® dsDNA HS Assay Kit (life technologies) and a fluorescence plate reader (FLUOstar Omega, BMG Labtech, Germany). Enzymatic conversion was performed using the NEBNext Enzymatic Methyl-seq Conversion Module (New England BioLabs, Cat#E7125S) according to the manufacturer's protocol.

**Whole-genome enzymatic methylation sequencing**

EM-seq libraries were prepared from sorted testicular germ cells of CTR and CZ samples (n=21) using 10-200 ng of DNA supplemented with 0.01% Lambda-/ 0.001% PUC-DNA. DNA was fragmented using the Bioruptor with 3 cycles of 30s on/ 90s off, and the library was prepared with 4-8 PCR cycles. The libraries were sequenced in a NovaSeq6000 instrument using a paired-end 2x150bp protocol and aiming for 80 Gb/sample.

**Data processing and EM-seq data analysis**

We processed the raw sequencing data using the wg-blimp pipeline (v 0.10.0) (Wöste *et al*, 2020) (Supplementary Table S10). Originally designed as a pipeline for analyzing whole-

genome-bisulfite-sequencing data, wg-blimp is also capable to handle enzymatic sequencing data, which shares the same raw data format but offers improved sequencing accuracy and reliability (Feng *et al*, 2020). wg-blimp incorporates the well-established algorithms for tasks such as bwa-meth for alignment (Li, 2013), MultiQC for quality control (Ewels *et al*, 2016), MethylDackl (v 0.6.1) (Ryan, 2021) for methylation calling, and camel (v 0.4.7) (Schröder, 2018) and metilene (v 0.2-8) (Jühling *et al*, 2016) for identifying DMRs. All data were aligned against the GRCh38.p7 reference genome.

To visualize the distribution of DNA methylation across various functional regions, we utilized the annotation sources provided by wg-blimp for hg38 alignment, which includes gtf-annotation and masked repeats. These alignments were imported into R 4.2.1 (R Core Team, 2022) using the *"rtracklayer"* (v 1.58.0) (Lawrence *et al*, 2009), while the identification of methylated regions of interest was performed using the *"GenomicRanges"* package (v 1.50.2) (Lawrence *et al*, 2013). Statistical analyses and graph plotting were performed using R packages, namely *"stats"* (v 4.2.1), *"ggplot2"* (v 3.3.6) (Wickham, 2016), and *"introdataviz*" (v 0.0.0.9003) (Nordmann *et al*, 2022). For the analysis of methylation distribution, we considered only CpG sites with a minimum coverage of 5.

Principal component analysis (PCA) was conducted on the methylation values, which were obtained from the wg-blimp software using the tool MethylDackl. The PCA analysis was conducted on 2521 CpG sites within the 50 known imprinted control regions (ICRs) (Monk *et al*, 2018), where all samples exhibited at least 5 x coverage.

**DMR analyses**

DMR calling was conducted using the wg-blimp software. The following criteria for DMR identification were applied: A minimum coverage of 5 per CpG loci, covering at least 5 CpG sites within a DMR, showing at least 20% methylation difference in the compared groups, and a maximum mean difference of ≤ 30% within each group for the CTR samples and ≤

15% for the CZ samples, to reduce the influence of genetic variability between patients. For metilene, a threshold of q < 0.05 was set, whereas camel uses t-statistics for verification.

Positive or negative enrichment of DMRs within specific genomic regions was assessed using permutation tests. The regions of interest were annotated using R 4.3.0 (R Core Team, 2023) with the packages “stats” (v 4.3.0), "*annotatR*" (Cavalcante & Sartor, 2017) and *"TxDb.Hsapiens.UCSC.hg38.knownGene"* (v 3.17.0) (Team BC & Maintainer BP, 2019), while the masked repeats were annotated using the annotation provided by wg-blimp. Permutation tests were performed using *"regioneR"* (Gel *et al*, 2016) and "*GenomicRanges*" using a Bonferroni correction (α=0.00019). Differences were quantified using z-scores and p-values provided by the permutation test with 10,000 iterations in *"regioneR"*.

To evaluate the average expression and percentage of cells expressing the DMR associated genes identified in this study, we used a previously published dataset (Di Persio *et al*, 2021b). Evaluation was performed using Seurat (Stuart *et al*, 2019; Hao *et al*, 2021). For better comparison to our dataset, we summarized the spermatocyte and spermatid cells from the scRNA-seq dataset together. Germ cell type-specific genes for undifferentiated spermatogonia, differentiating spermatogonia, spermatocytes, and spermatids were extracted based on differential gene expression analysis using MAST (Finak *et al*, 2015). Filtration criteria for germ cell type-specific genes were: log fold change threshold of ≥ 0.5, FDR-corrected p-value below 0.01 and expression in at least 25% of the cells of one comparison group.

**GO term analyses**

*“ChIPseeker”* (Yu *et al*, 2015) was used to retrieve a comprehensive gene list of overlapping genes, gene promoters (TSS ± 1000 bp) and flanking genes (putative regulatory sites, 5000 bp) from our DMRs. These comprehensive DMR associated gene lists were then analyzed for GO term enrichment for BP, MF, and CC using *“clusterProfiler”* (Wu *et al*, 2021) and the

enrichR database (Xie *et al*, 2021). P-Value was adjusted for multiple testing with Benjamini-Hochberg correction.

**Motif analysis**

To identify enriched known motifs of genes and TFs within the DMRs, we used HOMER (v 4.11) (Heinz *et al*, 2010). This tool was utilized with the default parameter of the fragments size of 200 bp and with the "-mask" parameter to use the repeat-masked sequences. Notably, HOMER uses regions with the same GC-content distribution as control.

**Retrieval of public datasets**

We downloaded the GSE40195 dataset from the GEO database, which contains ChIP-seq data of enriched regions for retained histones (H3.3, H3K14ac, H3K27ac, H3K36me3, H3K4me1 and H3K9me3) in human sperm. The data was converted to GRCh38/hg19 using "*rtracklayer"*.

**Statistical analyses**

Statistical analyses was performed as described in sections for data processing and EM-seq data analyses, DMR analysis, genomic annotation of the DMRs, and motif analysis.

## Data availability

EM-seq data has been deposited in the European Genome-Phenome Archive under EGAS00001007449.

# Supplemental information titles and legends

**Supplementary Fig. S1: Sorting strategy and quality check of sorted cells. A** Sorting strategy for the different germ cell types represented by 100,000 cells in the IgG and 1 Mio cells in the antibodies stained cells. IgG control showed no positive signal for MAGEA4 within the 2C cells and no signal for UTF1 and DMRT1 within the 2C/MAGEA4+ cells. **B** Box plots display methylation of sperm and blood (Laurentino *et al*, 2020) and each CTR sample in 2,761 sperm-soma DMRs of which 121 are hypermethylated and 2,640 are hypomethylated in sperm. Data are represented as median (center line), upper/ lower quartiles (box limits), 1.5 x interquartile range (whiskers).

**Supplementary Fig. S2: GO term enrichment analysis of biological process, molecular function and cellular components of the CTR DMRs.** All DMR group comparisons were compared and significant results of the top 8 terms with the lowest p-values are displayed. P-values were adjusted for multiple testing with Benjamini-Hochberg correction.

**Supplementary Fig. S3: DMR associated genes with germ cell type-specific expression. A** Hypermethylated and **B** hypomethylated DMR associated genes of the different group comparisons with specific expression in the respective germ cell types (Di Persio *et al*, 2021b) are depicted in dot plots. SPC = spermatocytes, SPD = spermatids.

**Supplementary Fig. S4: Purity check of the cryptozoospermic samples and features of CTR/CZ DMR associated genes. A** Box plots display methylation of sperm and blood (Laurentino *et al*, 2020) and each CZ sample in 2,761 sperm-soma DMRs. **B** Principal component analysis (PCA) of 2521 CpGs of the ICRs depicts clustering of all CTR samples and CZ-2 and CZ-3 samples together with sperm, whereas CZ-1 clustered towards blood, explaining 62.96% of variance (PC1). **C** Lineplots show the mean methylation in the 50 ICRs (Supplementary Table S6) for CZ-2 and CZ-3 in undifferentiated spermatogonia, differentiating spermatogonia, and primary spermatocytes compared to blood and sperm

631 samples (Laurentino *et al*, 2020). Box plots display the methylation of MKRN3:TSS-DMR in
632 the respective cell types. Data are represented as median (center line), upper/ lower
633 quartiles (box limits), 1.5 x interquartile range (whiskers). **D** Piecharts show the annotation of
634 the CTR/CZ DMRs for genes, promoters and intergenic regions. **E** GO term enrichment
635 analysis for biological processes in the CTR/CZ DMRs. The top 5 results are shown. **F** Dot
636 plots showing DMR associated genes with germ cell-type specific expression (Di Persio *et al*,
637 2021b). Genes marked with asterics are present in more than one group. SPC =
638 spermatocytes, SPD = spermatids Panel A created with BioRender.com.

639

640 **Supplementary Fig. S5: DNA methylation levels of TEs per CTR and CZ samples.** Violin
641 plots showing the CpG methylation of evolutionarily younger (white boxes: L1Hs, L1PA2-5,
642 and SVA A/B/C/D/E/F) and older (grey boxes: HERVH-int and L1M7) TEs per CTR and CZ
643 samples.

# References

Aravin AA, Sachidanandam R, Girard A, Fejes-Toth K & Hannon GJ (2007) Developmentally Regulated piRNA Clusters Implicate MILI in Transposon Control. *Science* 316: 744–747

Åsenius F, Danson AF & Marzi SJ (2020) DNA methylation in human sperm: a systematic review. *Human Reproduction Update* 26: 841–873

Ball MP, Li JB, Gao Y, Lee J-H, LeProust EM, Park I-H, Xie B, Daley GQ & Church GM (2009) Targeted and genome-scale strategies reveal gene-body methylation signatures in human cells. *Nat Biotechnol* 27: 361–368

Barau J, Teissandier A, Zamudio N, Roy S, Nalesso V, Hérault Y, Guillou F & Bourc'his D (2016) The DNA methyltransferase DNMT3C protects male germ cells from transposon activity. *Science* 354: 909–912

Bergmann M & Kliesch S (2010) Testicular biopsy and histology. In: Nieschlag E., Behre H.M., and Nieschlag S. (eds) Andrology Berlin, Heidelberg: Springer

Bourc'his D & Bestor TH (2004) Meiotic catastrophe and retrotransposon reactivation in male germ cells lacking Dnmt3L. *Nature* 431: 96–99

Bourc'his D, Xu G-L, Lin C-S, Bollman B & Bestor TH (2001) Dnmt3L and the Establishment of Maternal Genomic Imprints. *Science* 294: 2536–2539

Brykczynska U, Hisano M, Erkek S, Ramos L, Oakeley EJ, Roloff TC, Beisel C, Schübeler D, Stadler MB & Peters AHFM (2010) Repressive and active histone methylation mark distinct promoters in human and mouse spermatozoa. *Nat Struct Mol Biol* 17: 679–687

Carmell MA, Girard A, van de Kant HJG, Bourc'his D, Bestor TH, de Rooij DG & Hannon GJ (2007) MIWI2 Is Essential for Spermatogenesis and Repression of Transposons in the Mouse Male Germline. *Developmental Cell* 12: 503–514

Cavalcante RG & Sartor MA (2017) annotatr: genomic regions in context. *Bioinformatics* 33: 2381–2383

De Fazio S, Bartonicek N, Di Giacomo M, Abreu-Goodger C, Sankar A, Funaya C, Antony C, Moreira PN, Enright AJ & O'Carroll D (2011) The endonuclease activity of Mili fuels piRNA amplification that silences LINE1 elements. *Nature* 480: 259–263

Di Persio S, Leitão E, Wöste M, Tekath T, Cremers J-F, Dugas M, Li X, Meyer zu Hörste G, Kliesch S, Laurentino S, *et al* (2021a) Whole-genome methylation analysis of testicular germ cells from cryptozoospermic men points to recurrent and functionally relevant DNA methylation changes. *Clin Epigenet* 13: 160

Di Persio S, Tekath T, Siebert-Kuss LM, Cremers J-F, Wistuba J, Li X, Meyer zu Hörste G, Drexler HCA, Wyrwoll MJ, Tüttelmann F, *et al* (2021b) Single-cell RNA-seq unravels alterations of the human spermatogonial stem cell compartment in patients with impaired spermatogenesis. *Cell Rep Med* 2: 100395

Dong J, Wang X, Cao C, Wen Y, Sakashita A, Chen S, Zhang J, Zhang Y, Zhou L, Luo M, *et al* (2019) UHRF1 suppresses retrotransposons and cooperates with PRMT5 and PIWI proteins in male germ cells. *Nat Commun* 10: 4705

685 Dura M, Teissandier A, Armand M, Barau J, Lapoujade C, Fouchet P, Bonneville L, Schulz
686 M, Weber M, Baudrin LG, *et al* (2022) DNMT3A-dependent DNA methylation is
687 required for spermatogonial stem cells to commit to spermatogenesis. *Nat Genet* 54:
688 469–480

689 El Omri-Charai R, Gilbert I, Prunier J, Desmarais R, Ghinet MG, Robert C, Boissonneault G
690 & Delbes G (2023) DNA methylation dynamic in male rat germ cells during
691 gametogenesis. *Development* 150: dev201606

692 Ernst C, Eling N, Martinez-Jimenez CP, Marioni JC & Odom DT (2019) Staged
693 developmental mapping and X chromosome transcriptional dynamics during mouse
694 spermatogenesis. *Nat Commun* 10: 1251

695 Ewels P, Magnusson M, Lundin S & Käller M (2016) MultiQC: summarize analysis results for
696 multiple tools and samples in a single report. *Bioinformatics* 32: 3047–3048

697 Feng S, Zhong Z, Wang M & Jacobsen SE (2020) Efficient and accurate determination of
698 genome-wide DNA methylation patterns in Arabidopsis thaliana with enzymatic
699 methyl sequencing. *Epigenetics & Chromatin* 13: 42

700 Finak G, McDavid A, Yajima M, Deng J, Gersuk V, Shalek AK, Slichter CK, Miller HW,
701 McElrath MJ, Prlic M, *et al* (2015) MAST: a flexible statistical framework for assessing
702 transcriptional changes and characterizing heterogeneity in single-cell RNA
703 sequencing data. *Genome Biol* 16: 278

704 Gaysinskaya V, Miller BF, De Luca C, van der Heijden GW, Hansen KD & Bortvin A (2018)
705 Transient reduction of DNA methylation at the onset of meiosis in male mice.
706 *Epigenetics & Chromatin* 11: 15

707 Gel B, Díez-Villanueva A, Serra E, Buschbeck M, Peinado MA & Malinverni R (2016)
708 regioneR: an R/Bioconductor package for the association analysis of genomic regions
709 based on permutation tests. *Bioinformatics* 32: 289–291

710 Gkountela S, Zhang KX, Shafiq TA, Liao W-W, Hargan-Calvopiña J, Chen P-Y & Clark AT
711 (2015) DNA Demethylation Dynamics in the Human Prenatal Germline. *Cell* 161:
712 1425–1436

713 Greenberg MVC & Bourc'his D (2019) The diverse roles of DNA methylation in mammalian
714 development and disease. *Nat Rev Mol Cell Biol* 20: 590–607

715 Guo F, Yan L, Guo H, Li L, Hu B, Zhao Y, Yong J, Hu Y, Wang X, Wei Y, *et al* (2015) The
716 Transcriptome and DNA Methylome Landscapes of Human Primordial Germ Cells.
717 *Cell* 161: 1437–1452

718 Hammoud SS, Nix DA, Zhang H, Purwar J, Carrell DT & Cairns BR (2009) Distinctive
719 chromatin in human sperm packages genes for embryo development. *Nature* 460:
720 473–478

721 Hao Y, Hao S, Andersen-Nissen E, Mauck WM, Zheng S, Butler A, Lee MJ, Wilk AJ, Darby
722 C, Zager M, *et al* (2021) Integrated analysis of multimodal single-cell data. *Cell* 184:
723 3573-3587.e29

724 Heinz S, Benner C, Spann N, Bertolino E, Lin YC, Laslo P, Cheng JX, Murre C, Singh H &
725 Glass CK (2010) Simple Combinations of Lineage-Determining Transcription Factors
726 Prime cis-Regulatory Elements Required for Macrophage and B Cell Identities.
727 *Molecular Cell* 38: 576–589

728 Heyn H, Ferreira HJ, Bassas L, Bonache S, Sayols S, Sandoval J, Esteller M & Larriba S
729 (2012) Epigenetic Disruption of the PIWI Pathway in Human Spermatogenic
730 Disorders. *PLoS ONE* 7: e47892

731 Huang Y, Li L, An G, Yang X, Cui M, Song X, Lin J, Zhang X, Yao Z, Wan C, *et al* (2023)
732 Single-cell multi-omics sequencing of human spermatogenesis reveals a DNA
733 demethylation event associated with male meiotic recombination. *Nat Cell Biol* 25:
734 1520–1534

735 Izzo F, Lee SC, Poran A, Chaligne R, Gaiti F, Gross B, Murali RR, Deochand SD, Ang C,
736 Jones PW, *et al* (2020) DNA methylation disruption reshapes the hematopoietic
737 differentiation landscape. *Nat Genet* 52: 378–387

738 Jühling F, Kretzmer H, Bernhart SH, Otto C, Stadler PF & Hoffmann S (2016) metilene: fast
739 and sensitive calling of differentially methylated regions from bisulfite sequencing
740 data. *Genome Res* 26: 256–262

741 Karahan G, Chan D, Shirane K, McClatchie T, Janssen S, Baltz JM, Lorincz M & Trasler J
742 (2021) Paternal MTHFR deficiency leads to hypomethylation of young
743 retrotransposons and reproductive decline across two successive generations.
744 *Development* 148: dev199492

745 Kläver R, Tüttelmann F, Bleiziffer A, Haaf T, Kliesch S & Gromoll J (2013) DNA methylation
746 in spermatozoa as a prospective marker in andrology. *Andrology* 1: 731–740

747 Klemm SL, Shipony Z & Greenleaf WJ (2019) Chromatin accessibility and the regulatory
748 epigenome. *Nat Rev Genet* 20: 207–220

749 Kobayashi H, Sakurai T, Imai M, Takahashi N, Fukuda A, Yayoi O, Sato S, Nakabayashi K,
750 Hata K, Sotomaru Y, *et al* (2012) Contribution of Intragenic DNA Methylation in
751 Mouse Gametic DNA Methylomes to Establish Oocyte-Specific Heritable Marks.
752 *PLoS Genet* 8: e1002440

753 Kubo N, Toh H, Shirane K, Shirakawa T, Kobayashi H, Sato T, Sone H, Sato Y, Tomizawa S,
754 Tsurusaki Y, *et al* (2015) DNA methylation and gene expression dynamics during
755 spermatogonial stem cell differentiation in the early postnatal mouse testis. *BMC*
756 *Genomics* 16: 624

757 Kuhtz J, Schneider E, El Hajj N, Zimmermann L, Fust O, Linek B, Seufert R, Hahn T,
758 Schorsch M & Haaf T (2014) Epigenetic heterogeneity of developmentally important
759 genes in human sperm: Implications for assisted reproduction outcome. *Epigenetics*
760 9: 1648–1658

761 Lambrot R, Chan D, Shao X, Aarabi M, Kwan T, Bourque G, Moskovtsev S, Librach C,
762 Trasler J, Dumeaux V, *et al* (2021) Whole-genome sequencing of H3K4me3 and DNA
763 methylation in human sperm reveals regions of overlap linked to fertility and
764 development. *Cell Reports* 36: 109418

765 Langenstroth-Röwer D, Gromoll J, Wistuba J, Tröndle I, Laurentino S, Schlatt S & Neuhaus
766 N (2017) De novo methylation in male germ cells of the common marmoset monkey
767 occurs during postnatal development and is maintained in vitro. *Epigenetics* 12: 527–
768 539

769 Laurentino S, Beygo J, Nordhoff V, Kliesch S, Wistuba J, Borgmann J, Buiting K,
770 Horsthemke B & Gromoll J (2015) Epigenetic germline mosaicism in infertile men.
771 *Human Molecular Genetics* 24: 1295–1304

772 Laurentino S, Cremers J, Horsthemke B, Tüttelmann F, Czeloth K, Zitzmann M, Pohl E,
773 Rahmann S, Schröder C, Berres S, *et al* (2020) A germ cell-specific ageing pattern in
774 otherwise healthy men. *Aging Cell* 19: e13242

775 Lawrence M, Gentleman R & Carey V (2009) rtracklayer: an R package for interfacing with
776 genome browsers. *Bioinformatics* 25: 1841–1842

777 Lawrence M, Huber W, Pagès H, Aboyoun P, Carlson M, Gentleman R, Morgan MT & Carey
778 VJ (2013) Software for Computing and Annotating Genomic Ranges. *PLoS Comput*
779 *Biol* 9: e1003118

780 Leitão E, Di Persio S, Laurentino S, Wöste M, Dugas M, Kliesch S, Neuhaus N &
781 Horsthemke B (2020) The sperm epigenome does not display recurrent epimutations
782 in patients with severely impaired spermatogenesis. *Clin Epigenet* 12: 61

783 Li H (2013) Aligning sequence reads, clone sequences and assembly contigs with BWA-
784 MEM. arXiv preprint. arXiv:1303.3997. 2013. [PREPRINT]

785 Markenscoff-Papadimitriou E, Whalen S, Przytycki P, Thomas R, Binyameen F, Nowakowski
786 TJ, Kriegstein AR, Sanders SJ, State MW, Pollard KS, *et al* (2020) A Chromatin
787 Accessibility Atlas of the Developing Human Telencephalon. *Cell* 182: 754-769.e18

788 Marques CJ, Carvalho F, Sousa M & Barros A (2004) Genomic imprinting in disruptive
789 spermatogenesis. *The Lancet* 363: 1700–1702

790 Monk D, Morales J, den Dunnen JT, Russo S, Court F, Prawitt D, Eggermann T, Beygo J,
791 Buiting K, Tümer Z, *et al* (2018) Recommendations for a nomenclature system for
792 reporting methylation aberrations in imprinted domains. *Epigenetics* 13: 117–121

793 Nordmann E, McAleer P, Toivo W, Paterson H & DeBruine LM (2022) Data Visualization
794 Using R for Researchers Who Do Not Use R. *Advances in Methods and Practices in*
795 *Psychological Science* 5: 251524592210746

796 Oakes CC, La Salle S, Smiraglia DJ, Robaire B & Trasler JM (2007) Developmental
797 acquisition of genome-wide DNA methylation occurs prior to meiosis in male germ
798 cells. *Developmental Biology* 307: 368–379

799 Piovesan A, Pelleri MC, Antonaros F, Strippoli P, Caracausi M & Vitale L (2019) On the
800 length, weight and GC content of the human genome. *BMC Res Notes* 12: 106

801 Poplinski A, Tüttelmann F, Kanber D, Horsthemke B & Gromoll J (2010) Idiopathic male
802 infertility is strongly associated with aberrant methylation of *MEST* and *IGF2/H19*
803 *ICR1*. *International Journal of Andrology* 33: 642–649

804 R Core Team (2022) R: A Language and Environment for Statistical Computing. *R*
805 *Foundation for Statistical Computing, Vienna, Austria*

806 R Core Team (2023) R: A Language and Environment for Statistical Computing. *R*
807 *Foundation for Statistical Computing, Vienna, Austria*

808 Raiz J, Damert A, Chira S, Held U, Klawitter S, Hamdorf M, Löwer J, Strätling WH, Löwer R
809 & Schumann GG (2012) The non-autonomous retrotransposon SVA is trans -
810 mobilized by the human LINE-1 protein machinery. *Nucleic Acids Research* 40:
811 1666–1683

812 Ryan D (2021) MethylDackel.https://github.com/dpryan79/ methyldackel.

Sangrithi MN, Royo H, Mahadevaiah SK, Ojarikre O, Bhaw L, Sesay A, Peters AHFM, Stadler M & Turner JMA (2017) Non-Canonical and Sexually Dimorphic X Dosage Compensation States in the Mouse and Human Germline. *Developmental Cell* 40: 289-301.e3

Sasaki T, Nishihara H, Hirakawa M, Fujimura K, Tanaka M, Kokubo N, Kimura-Yoshida C, Matsuo I, Sumiyama K, Saitou N, *et al* (2008) Possible involvement of SINEs in mammalian-specific brain formation. *Proc Natl Acad Sci USA* 105: 4220–4225

Schaefer CB, Ooi SKT, Bestor TH & Bourc'his D (2007) Epigenetic Decisions in Mammalian Germ Cells. *Science* 316: 398–399

Schröder C (2018) Bioinformatics from genetic variants to methylation. https://eldorado.tu-dortmund.de/handle/2003/37940.

Seisenberger S, Andrews S, Krueger F, Arand J, Walter J, Santos F, Popp C, Thienpont B, Dean W & Reik W (2012) The Dynamics of Genome-wide DNA Methylation Reprogramming in Mouse Primordial Germ Cells. *Molecular Cell* 48: 849–862

Sharda A & Humphrey TC (2022) The role of histone H3K36me3 writers, readers and erasers in maintaining genome stability. *DNA Repair* 119: 103407

Siebert-Kuss LM, Krenz H, Tekath T, Wöste M, Di Persio S, Terwort N, Wyrwoll MJ, Cremers J-F, Wistuba J, Dugas M, *et al* (2023) Transcriptome analyses in infertile men reveal germ cell–specific expression and splicing patterns. *Life Sci Alliance* 6: e202201633

Soumillon M, Necsulea A, Weier M, Brawand D, Zhang X, Gu H, Barthès P, Kokkinaki M, Nef S, Gnirke A, *et al* (2013) Cellular Source and Mechanisms of High Transcriptome Complexity in the Mammalian Testis. *Cell Rep* 3: 2179–2190

Stadler MB, Murr R, Burger L, Ivanek R, Lienert F, Schöler A, Nimwegen E van, Wirbelauer C, Oakeley EJ, Gaidatzis D, *et al* (2011) DNA-binding factors shape the mouse methylome at distal regulatory regions. *Nature* 480: 490–495

Stuart T, Butler A, Hoffman P, Hafemeister C, Papalexi E, Mauck WM, Hao Y, Stoeckius M, Smibert P & Satija R (2019) Comprehensive integration of single-cell data. *Cell* 177: 1888-1902.e21

Team BC & Maintainer BP (2019) TxDb.Hsapiens.UCSC.hg38.knownGene: Annotation package for TxDb object(s).

Tüttelmann F, Ruckert C & Röpke A (2018) Disorders of spermatogenesis: Perspectives for novel genetic diagnostics after 20 years of unchanged routine. *medgen* 30: 12–20

Urdinguio RG, Bayón GF, Dmitrijeva M, Toraño EG, Bravo C, Fraga MF, Bassas L, Larriba S & Fernández AF (2015) Aberrant DNA methylation patterns of spermatozoa in men with unexplained infertility. *Human Reproduction* 30: 1014–1028

Vaissiere T, Sawan C & Herceg Z (2008) Epigenetic interplay between histone modifications and DNA methylation in gene silencing. *Mutation Research/Reviews in Mutation Research* 659: 40–48

Vasiliauskaitė L, Berrens RV, Ivanova I, Carrieri C, Reik W, Enright AJ & O'Carroll D (2018) Defective germline reprogramming rewires the spermatogonial transcriptome. *Nat Struct Mol Biol* 25: 394–404

Wickham H (2016) ggplot2: Elegant Graphics for Data Analysis Springer-Verlag New York,

World Health Organization (2010) WHO Laboratory Manual for the Examination and Processing of Human Semen World Health Organization

Wöste M, Leitão E, Laurentino S, Horsthemke B, Rahmann S & Schröder C (2020) wg-blimp: an end-to-end analysis pipeline for whole genome bisulfite sequencing data. *BMC Bioinformatics* 21: 169

Wu T, Hu E, Xu S, Chen M, Guo P, Dai Z, Feng T, Zhou L, Tang W, Zhan L, *et al* (2021) clusterProfiler 4.0: A universal enrichment tool for interpreting omics data. *The Innovation* 2: 100141

Xie Z, Bailey A, Kuleshov MV, Clarke DJB, Evangelista JE, Jenkins SL, Lachmann A, Wojciechowicz ML, Kropiwnicki E, Jagodnik KM, *et al* (2021) Gene Set Knowledge Discovery with Enrichr. *Current Protocols* 1: e90

Yu G, Wang L-G & He Q-Y (2015) ChIPseeker: an R/Bioconductor package for ChIP peak annotation, comparison and visualization. *Bioinformatics* 31: 2382–2383

Zamudio N, Barau J, Teissandier A, Walter M, Borsos M, Servant N & Bourc'his D (2015) DNA methylation restrains transposons from adopting a chromatin signature permissive for meiotic recombination. *Genes Dev* 29: 1256–1270

Zamudio N & Bourc'his D (2010) Transposable elements in the mammalian germline: a comfortable niche or a deadly trap? *Heredity* 105: 92–104

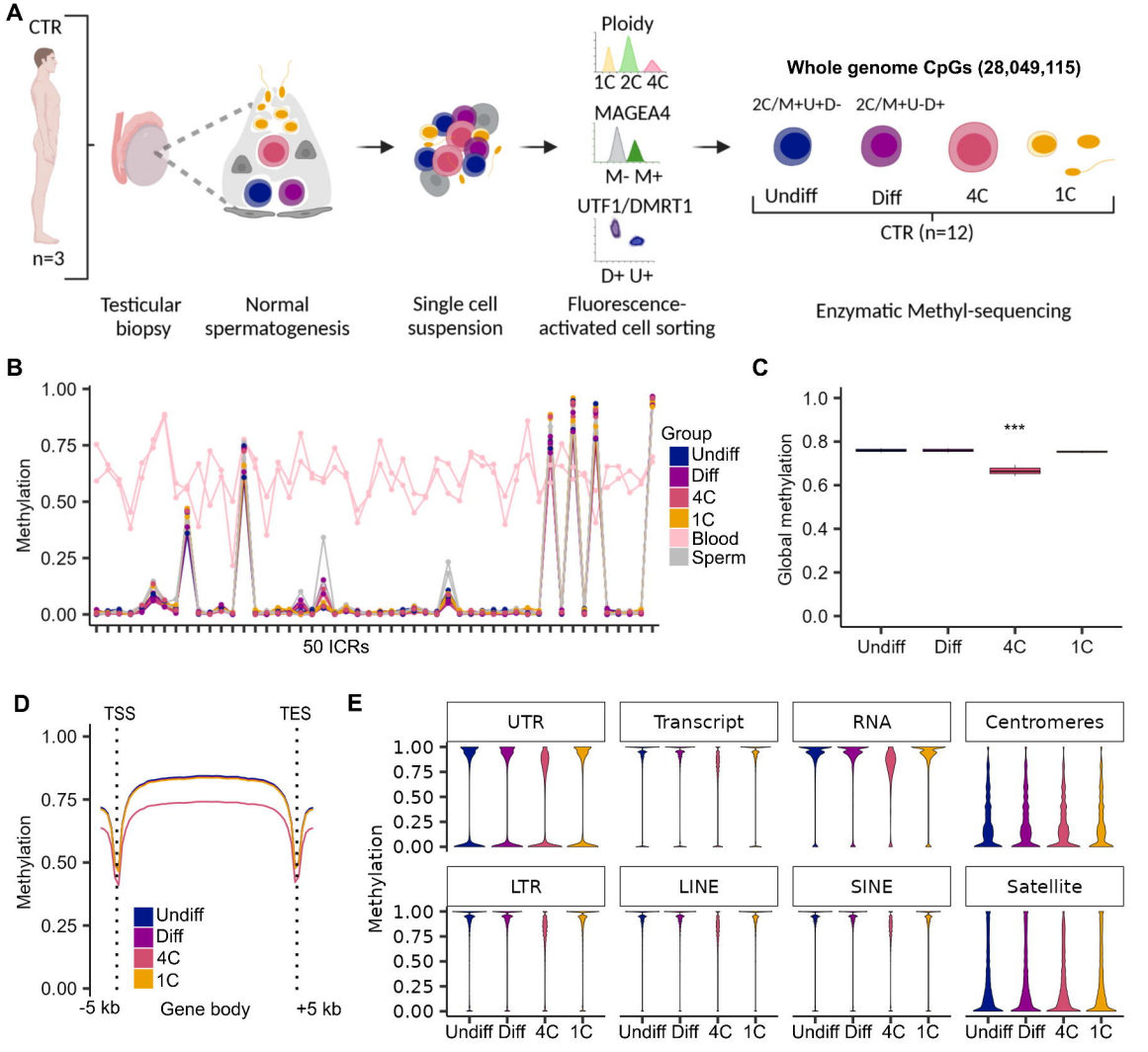
A
CTR
n=3
Testicular biopsy
Normal spermatogenesis
Single cell suspension
Ploidy
1C 2C 4C
MAGEA4
M- M+
UTF1/DMRT1
D+ U+
Fluorescence-activated cell sorting
Whole genome CpGs (28,049,115)
2C/M+U+D-
2C/M+U-D+
Undiff
Diff
4C
1C
CTR (n=12)
Enzymatic Methyl-sequencing
B
Methylation
50 ICRs
Group
Undiff
Diff
4C
1C
Blood
Sperm
C
Global methylation
***
Undiff
Diff
4C
1C
D
TSS
TES
Methylation
Undiff
Diff
4C
1C
-5 kb
Gene body
+5 kb
E
UTR
Transcript
RNA
Centromeres
LTR
LINE
SINE
Satellite
Methylation
Undiff Diff 4C 1C

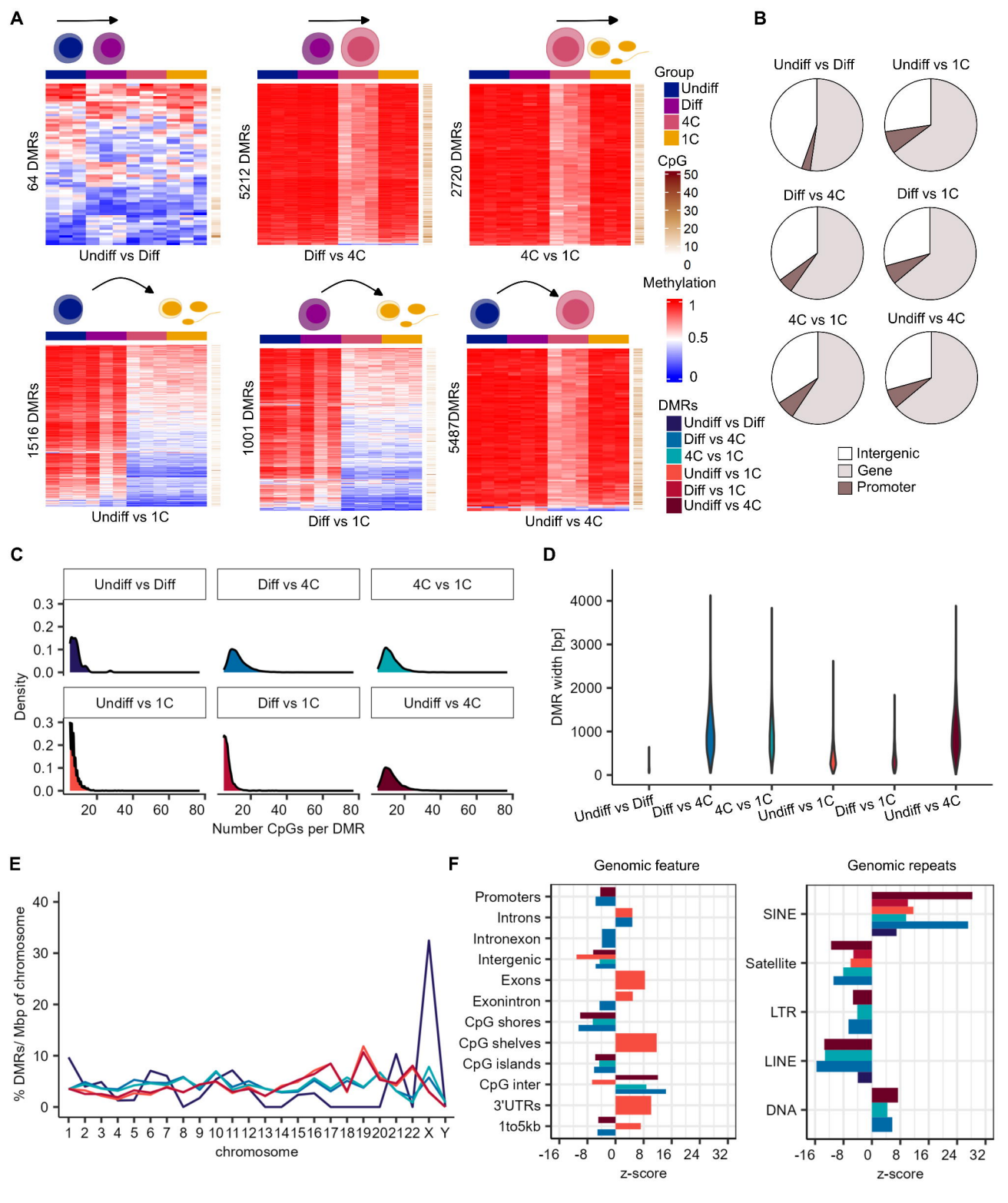
A
64 DMRs
Undiff vs Diff
5212 DMRs
Diff vs 4C
2720 DMRs
4C vs 1C
1516 DMRs
Undiff vs 1C
1001 DMRs
Diff vs 1C
5487DMRs
Undiff vs 4C
Group
Undiff
Diff
4C
1C
CpG
50
40
30
20
10
0
Methylation
1
0.5
0
DMRs
Undiff vs Diff
Diff vs 4C
4C vs 1C
Undiff vs 1C
Diff vs 1C
Undiff vs 4C
B
Undiff vs Diff
Undiff vs 1C
Diff vs 4C
Diff vs 1C
4C vs 1C
Undiff vs 4C
Intergenic
Gene
Promoter
C
Undiff vs Diff
Diff vs 4C
4C vs 1C
Undiff vs 1C
Diff vs 1C
Undiff vs 4C
Density
0.3
0.2
0.1
0.0
20
40
60
80
Number CpGs per DMR
D
DMR width [bp]
4000
3000
2000
1000
0
Undiff vs Diff
Diff vs 4C
4C vs 1C
Undiff vs 1C
Diff vs 1C
Undiff vs 4C
E
% DMRs/ Mbp of chromosome
40
30
20
10
0
1 2 3 4 5 6 7 8 9 10 11 12 13 14 15 16 17 18 19 20 21 22 X Y
chromosome
F
Genomic feature
Promoters
Introns
Intronexon
Intergenic
Exons
Exonintron
CpG shores
CpG shelves
CpG islands
CpG inter
3'UTRs
1to5kb
-16 -8 0 8 16 24 32
z-score
Genomic repeats
SINE
Satellite
LTR
LINE
DNA
-16 -8 0 8 16 24 32
z-score

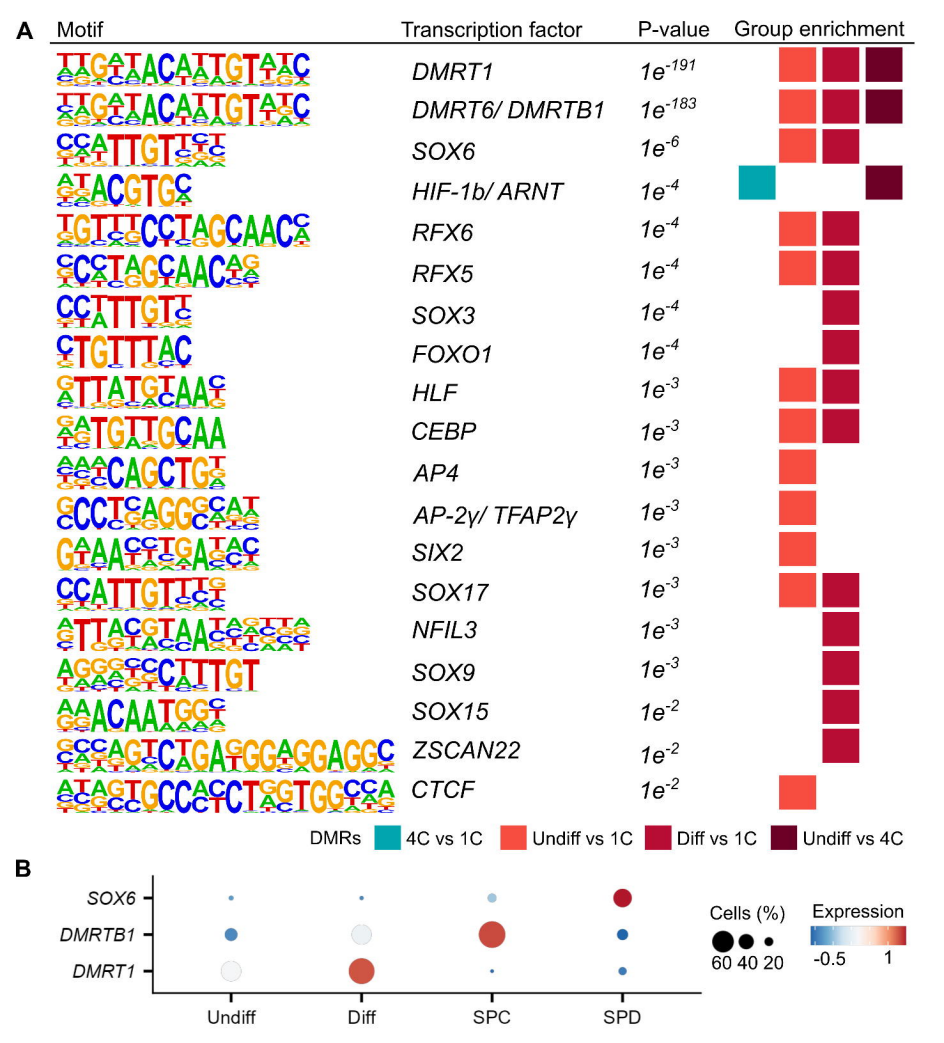
A
Motif
Transcription factor
P-value
Group enrichment
DMRT1
1e-191
DMRT6/ DMRTB1
1e-183
SOX6
1e-6
HIF-1b/ ARNT
1e-4
RFX6
1e-4
RFX5
1e-4
SOX3
1e-4
FOXO1
1e-4
HLF
1e-3
CEBP
1e-3
AP4
1e-3
AP-2γ/ TFAP2γ
1e-3
SIX2
1e-3
SOX17
1e-3
NFIL3
1e-3
SOX9
1e-3
SOX15
1e-2
ZSCAN22
1e-2
CTCF
1e-2
DMRs
4C vs 1C
Undiff vs 1C
Diff vs 1C
Undiff vs 4C
B
SOX6
DMRTB1
DMRT1
Undiff
Diff
SPC
SPD
Cells (%)
60 40 20
Expression
-0.5
1

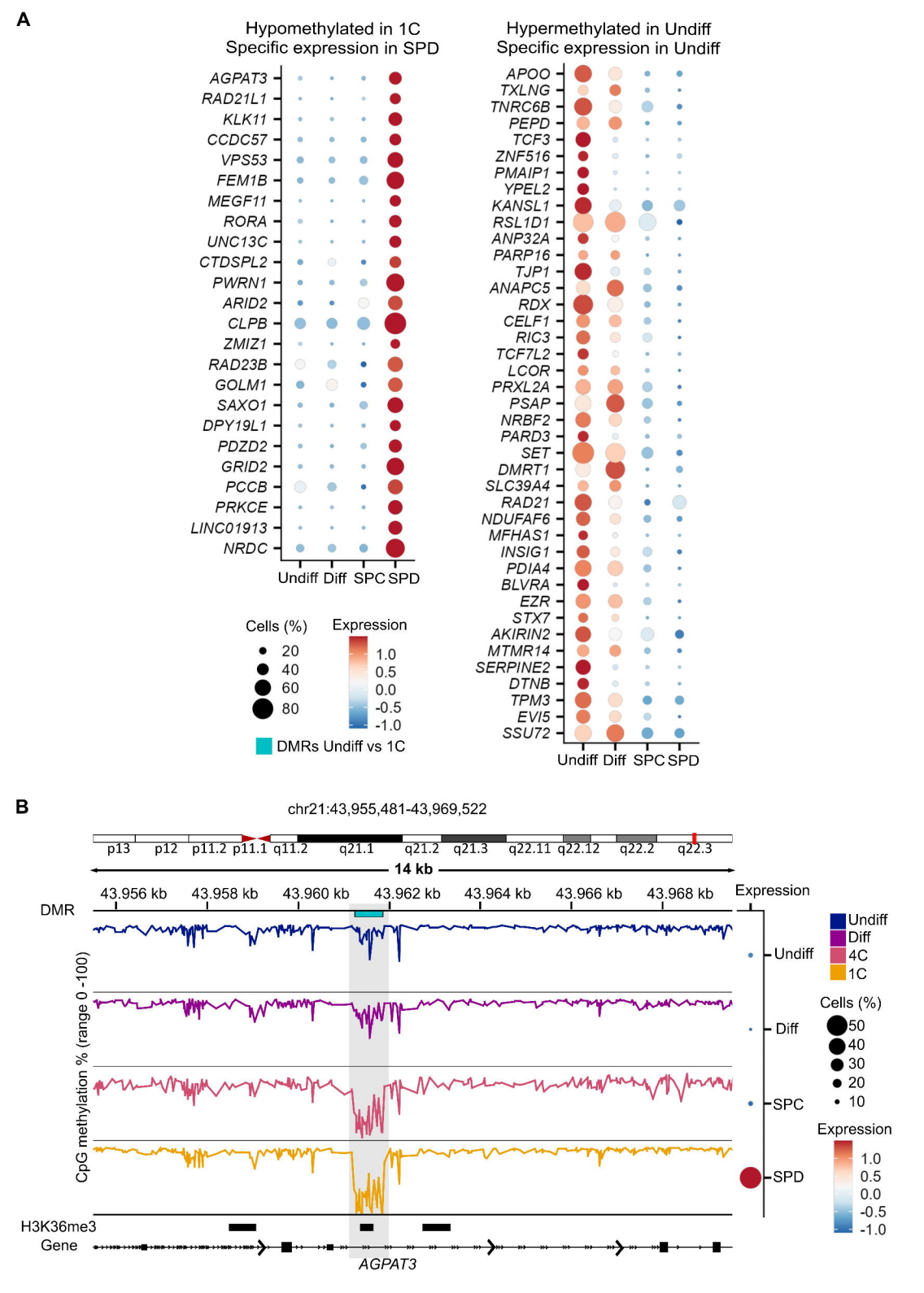
A
Hypomethylated in 1C
Specific expression in SPD
AGPAT3
RAD21L1
KLK11
CCDC57
VPS53
FEM1B
MEGF11
RORA
UNC13C
CTDSPL2
PWRN1
ARID2
CLPB
ZMIZ1
RAD23B
GOLM1
SAXO1
DPY19L1
PDZD2
GRID2
PCCB
PRKCE
LINC01913
NRDC
Undiff Diff SPC SPD
Hypermethylated in Undiff
Specific expression in Undiff
APOO
TXLNG
TNRC6B
PEPD
TCF3
ZNF516
PMAIP1
YPEL2
KANSL1
RSL1D1
ANP32A
PARP16
TJP1
ANAPC5
RDX
CELF1
RIC3
TCF7L2
LCOR
PRXL2A
PSAP
NRBF2
PARD3
SET
DMRT1
SLC39A4
RAD21
NDUFAF6
MFHAS1
INSIG1
PDIA4
BLVRA
EZR
STX7
AKIRIN2
MTMR14
SERPINE2
DTNB
TPM3
EVI5
SSU72
Undiff Diff SPC SPD
Cells (%)
20
40
60
80
Expression
1.0
0.5
0.0
-0.5
-1.0
DMRs Undiff vs 1C
B
chr21:43,955,481-43,969,522
p13 p12 p11.2 p11.1 q11.2 q21.1 q21.2 q21.3 q22.11 q22.12 q22.2 q22.3
14 kb
43.956 kb 43.958 kb 43.960 kb 43.962 kb 43.964 kb 43.966 kb 43.968 kb
DMR
CpG methylation % (range 0 -100)
H3K36me3
Gene
AGPAT3
Expression
Undiff
Diff
SPC
SPD
Undiff
Diff
4C
1C
Cells (%)
50
40
30
20
10
Expression
1.0
0.5
0.0
-0.5
-1.0

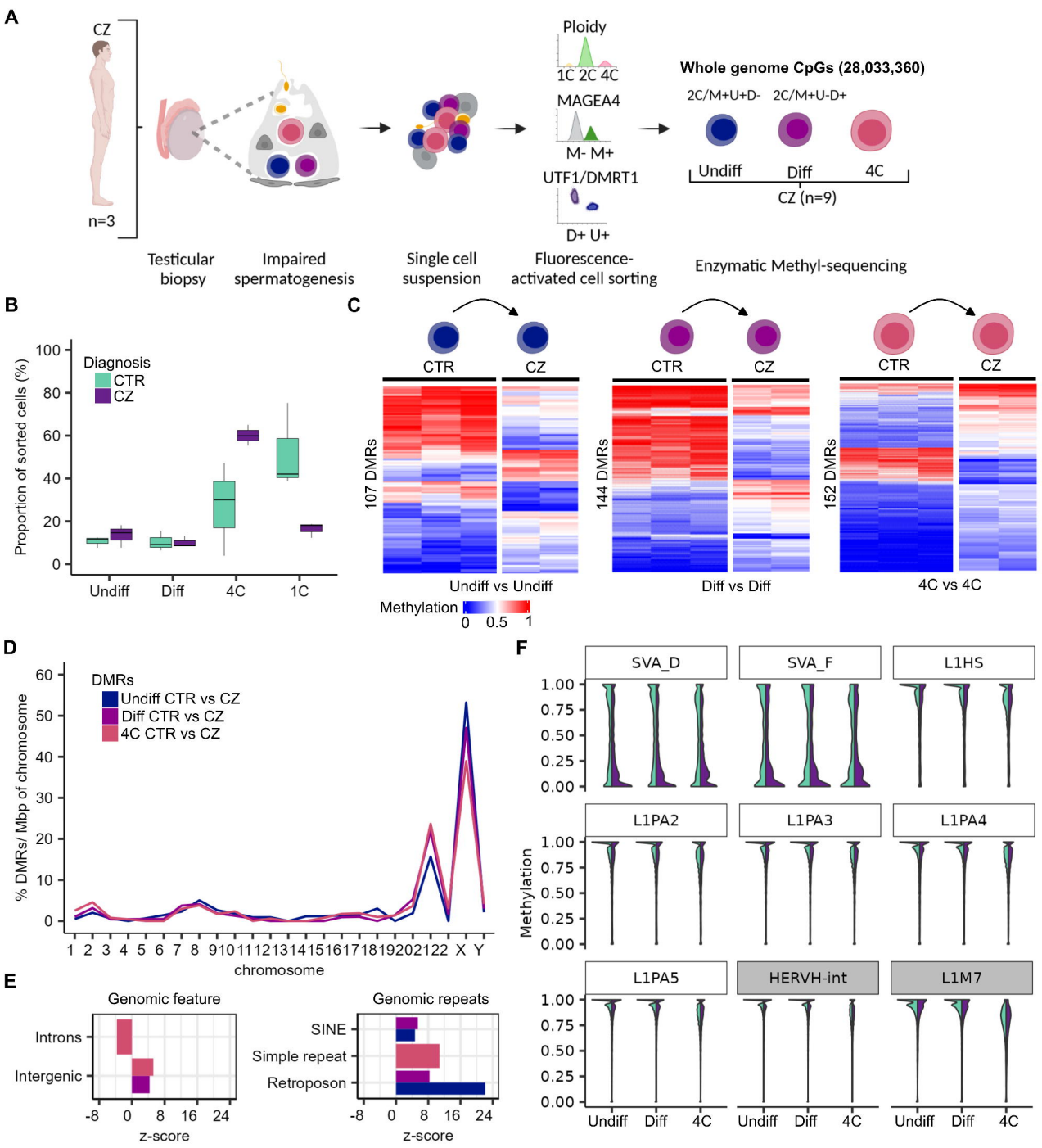
A
CZ
n=3
Testicular biopsy
Impaired spermatogenesis
Single cell suspension
Ploidy
1C 2C 4C
MAGEA4
M- M+
UTF1/DMRT1
D+ U+
Fluorescence-activated cell sorting
Whole genome CpGs (28,033,360)
2C/M+U+D-
2C/M+U-D+
Undiff
Diff
4C
CZ (n=9)
Enzymatic Methyl-sequencing
B
Proportion of sorted cells (%)
Diagnosis
CTR
CZ
Undiff
Diff
4C
1C
C
CTR
CZ
107 DMRs
144 DMRs
152 DMRs
Undiff vs Undiff
Diff vs Diff
4C vs 4C
Methylation
D
% DMRs/ Mbp of chromosome
DMRs
Undiff CTR vs CZ
Diff CTR vs CZ
4C CTR vs CZ
chromosome
E
Genomic feature
Introns
Intergenic
z-score
Genomic repeats
SINE
Simple repeat
Retroposon
z-score
F
SVA_D
SVA_F
L1HS
L1PA2
L1PA3
L1PA4
L1PA5
HERVH-int
L1M7
Methylation
Undiff
Diff
4C